Improving response and reducing toxicity to immune checkpoint blockade therapy in melanoma

Hoefsmit, E.P.

6

Systemic LRG1 expression in melanoma is associated with disease progression and recurrence

E. P. Hoefsmit[1,*], F. Völlmy[2,*], E. A. Rozeman[3], I. L. M. Reijers[3], J. M. Versluis[3], L. Hoekman[4], A. C. J. van Akkooi[5,6,7], G. V. Long[5,6,8,9], D. Schadendorf[10], R. Dummer[11], M. Altelaar[2,4,#], C. U. Blank[1,3,12#]

[*]Shared first author
[#] Corresponding authors

[1] Department of Molecular Oncology and Immunology, Netherlands Cancer Institute, Amsterdam, The Netherlands, [2] Biomolecular Mass Spectrometry and Proteomics, Center for Biomolecular Research and Utrecht Institute for Pharmaceutical Sciences, Utrecht University, Utrecht, The Netherlands, [3] Department of Medical Oncology, Netherlands Cancer Institute, Amsterdam, The Netherlands, [4] Proteomics Facility, Netherlands Cancer Institute, Amsterdam, The Netherlands, [5] Melanoma Institute Australia, The University of Sydney, Sydney, New South Wales, Australia, [6] Faculty of Medicine & Health, The University of Sydney, Sydney, New South Wales, Australia, [7] Department of Melanoma and Surgical Oncology, Royal Prince Alfred Hospital, Sydney, New South Wales, Australia, [8] Charles Perkins Centre, The University of Sydney, Sydney, New South Wales, Australia, [9] Department of Medical Oncology, Royal North Shore and Mater Hospitals, Sydney, New South Wales, Australia, [10] Department of Dermatology, University Hospital Essen & Germany Cancer Consortium, Partner Site Essen, Essen, Germany, [11] Department of Dermatology, University Hospital Zürich, University Zürich, Zürich, Switzerland, [12] Department of Medical Oncology, Leiden University Medical Center, Leiden, The Netherlands

Cancer Research Communications, 2023. Apr; 3(4): 672-683.
doi: 10.1158/2767-9764.CRC-23-0015

Abstract

The response rates upon neoadjuvant immune checkpoint blockade (ICB) in stage III melanoma are higher as compared to stage IV disease. Given that successful ICB depends on systemic immune response, we hypothesized that systemic immune suppression might be a mechanism responsible for lower response rates in late-stage disease, and also potentially with disease recurrence in early-stage disease. Plasma and serum samples of cohorts of melanoma patients were analyzed for circulating proteins using mass spectrometry proteomic profiling and Olink proteomic assay. A cohort of paired samples of patients with stage III that progressed to stage IV disease (n=64) was used to identify markers associated with higher tumor burden. Baseline patient samples from the OpACIN-neo study (n=83) and PRADO study (n=49; NCT02977052) were used as two independent cohorts to analyze whether the potential identified markers are also associated with disease recurrence after neoadjuvant ICB therapy. When comparing baseline proteins overlapping between patients with progressive disease and patients with recurrent disease, we found leucine-rich alpha-2-glycoprotein 1 (LRG1) to be associated with worse prognosis. Especially non-responder patients to neoadjuvant ICB (OpACIN-neo) with high LRG1 expression had a poor outcome with an estimated 36-month event-free survival of 14% as compared to 83% for non-responders with a low LRG1 expression ($P = 0.014$). This finding was validated in an independent cohort ($P = 0.0021$). LRG1 can be used as a biomarker to identify patients with high risk for disease progression and recurrence, and might be a target to be combined with neoadjuvant ICB.

Significance

Leucine-rich alpha-2-glycoprotein 1 (LRG1) could serve as a potential target and as a biomarker to identify patients with high risk for disease recurrence, and consequently benefit from additional therapies and intensive follow-up.

Introduction

Immune checkpoint blockade using anti-programmed cell death 1 (anti-PD-1) antibodies, either as monotherapy, or in combination with anti-cytotoxic T-lymphocyte-associated protein 4 (anti-CTLA-4) antibodies, is currently one of the most effective standard therapies for late-stage melanoma (1, 2, 3, 4, 5). In cross-trial comparison, a higher response rate to ICB is observed for patients with stage III as compared to stage IV disease (5, 6, 7, 8). In addition, high grade (grade 3-4) immunotherapy-related adverse events (irAE) are more frequently observed in stage III melanoma than would be predicted from prior data in stage IV melanoma at similar dosing of ipilimumab 3 mg kg^{-1} plus nivolumab 1 mg kg^{-1} and number of courses (90% in stage III versus 59% in stage IV) (5, 6). The lower response rate and the lower irAE rates suggest that late-stage melanoma patients may have a higher level of systemic tumor associated immune suppression hampering ICB therapy (9).

The theory of systemic immune suppression is supported by analyses of immunocompetence showing that the proliferative capacity of peripheral lymphocytes decreases with disease progression (10). Given that successful ICB is reliant upon a systemic immune response (9), additional probing of this immune modulation could be beneficial to improve our understanding of the underlying lower response rate to ICB therapy in more advanced disease. Previous systemic proteomic biomarker analysis to distinguish early- and late-stage patients already identified few markers, including S100B, lactate dehydrogenase (LDH), C-reactive protein (CRP) and serum amyloid A (SAA) (11, 12, 13, 14, 15). A remaining challenge is to identify low-level abundant proteins biomarkers for disease progression and recurrence.

This prompted us to analyze a cohort of melanoma patients for circulating proteins using mass spectrometry-based protein profiling in an unbiased approach (16, 17). In this study, we analyzed serum of melanoma patients to identify systemic biomarkers that are associated with disease progression and recurrence in early-stage disease.

Material and methods

Study population

Melanoma patients with stage III melanoma that progressed to stage IV melanoma, from whom plasma/serum samples were available at both time points and were systemic treatment naïve at collection, were identified from four different cancer centers (Netherlands Cancer Institute (NKI), University Clinic Essen, University Hospital of Zürich and Melanoma Institute Australia (MIA)). Due to plasma/serum mismatches (samples within a patient) and heterogeneity between samples from European centers

and MIA, we finally analyzed a more homogeneous cohort of paired serum samples from patients from the NKI (n=5), University Clinic Essen (n=28) and University Hospital of Zürich (n=32). For serum sampling, blood was collected, spun down immediately after isolation and serum was harvested, snap-frozen and stored. These paired stage III melanoma and stage IV melanoma serum samples were used to determine difference in soluble factors by mass spectrometry-based proteomic analysis (n=64) and proximity extension assay (n=33; Olink Bioscience AB) (**Figure 1**).

In another cohort of patients, only plasma samples were available for mass spectrometry-based proteomic analysis. This cohort included patients treated with ICB to determine difference in soluble factors between patients with and without a disease recurrence after ICB treatment. Plasma was obtained from whole blood collected in Ethylene Diamine Tetra Acetic acid (EDTA) tubes and stored at -80°C after spinning. This cohort included baseline (pre-treatment) samples (n=83 patients) and post-treatment (week 6) samples (n=83 patients) of the OpACIN-neo study (NCT02977052) (**Figure S1**). Hematology (including white blood cell differentiation) was tested baseline (pre-treatment). The OpACIN-neo study tested three different dosing schedules of neoadjuvant ipilimumab plus nivolumab in stage III melanoma (A: two cycles ipilimumab 3 mg kg^{-1} plus nivolumab 1 mg kg^{-1} every 3 weeks; B: two cycles ipilimumab 1 mg kg^{-1} plus nivolumab 3 mg kg^{-1} every 3 weeks; C: two cycles ipilimumab 3 mg kg^{-1} every 3 weeks directly followed by two cycles nivolumab 3 mg kg^{-1} every 2 weeks) (7, 18).

To evaluate if the findings of the proximity extension assay (Olink Bioscience AB) could be confirmed in an independent cohort, pre-treatment plasma samples from patients with stage IV melanoma (n=22 patients) were collected at the NKI and compared to pre-treatment plasma samples from patients with stage III melanoma from the OpACIN-neo study (n=86 patients) (**Figure 1**). The study was approved by the Institutional Review Board of the NKI.

For validation cohort, baseline (pre-treatment) plasma samples of the PRADO study (n=49) were selected (8) (**Figure S2**). In this study, patients were also treated with neoadjuvant ipilimumab and nivolumab. The studies were conducted in accordance with Good Clinical Practice guidelines as defined by the International Conference of Harmonization and Declaration of Helsinki.

Ethics approval

All retrospective medical data/biospecimen studies at the Netherlands Cancer Institute have been executed pursuant to Dutch legislation and international standards (reference CFMPB558, N03LAM, OpACIN-neo, PRADO). Prior to May 25, 2018, national legislation on data protection applied, as well as the International Guideline on Good

Clinical Practice. From May 25, 2019, we also adhere to the GDPR. Within this framework, patients are informed and have always had the opportunely to object or actively consent to the (continued) use of their personal data and biospecimens in research. Hence the procedure comply both with (inter-)national legislative and ethical standards. All University Hospital Essen & Germany Cancer Consortium patient samples included in this study were collected covered by EC vote BO-11-4715 (Essen) with written consent. All University Hospital Zürich patient samples have signed a release form, which have been approved by the ethics committee and assigned the numbers EK647 and EK800.

Sample preparation for proteomic analysis of stage III and stage IV patients

For the serum samples, total protein concentration was determined using a Bradford assay and 600 mg worth of protein was loaded onto a Pierce Top 12 Abundant Protein Depletion Spin column (Thermo Fisher Scientific), followed by a 1-hour end-on-end rotating incubation at room temperature. The depleted serum was collected by centrifuging for 2 minutes at 1000G and each sample was split in two to generate parallel workflow duplicates. A detergent-based buffer (1% SDC, 10 mM TCEP, 10mM Tris, 40 mM chloroacetamide) with Complete mini EDTA-free protease inhibitor cocktail (Roche) was added to enhance protein denaturation and boiled for 5 minutes at 95°C. 50 mM ammonium bicarbonate was added and digestion was allowed to proceed overnight at 37°C using trypsin (Promega, Madison, WI, USA) and LysC (Wako, Richmond, VA, USA) at 1:50 and 1:75 enzyme:substrate ratios, respectively. The digestion was quenched with 10% formic acid and the resulting peptides were cleaned-up using Oasis HLB 96-well uElution plates (Waters Corporation, Milford, MA). The eluate was dried and resolubilized in 1% FA achieving a concentration of 1 mg/mL. HRM iRT retention time peptides (Biognosys) were spiked in following the producer's recommendations and finally an on-column peptide load of 1.5 mg peptides was achieved.

Sample preparation for proteomic analysis of OpACIN-neo and PRADO plasma

To enhance protein denaturation, 24 µl of a detergent-based buffer (1% sodium deoxycholate (SDC), 10 mM tris(2-carboxyethyl)phosphine (TCEP), 10 mM Tris, and 40 mM chloroacetamide) with Complete mini EDTA-free protease inhibitor cocktail (Roche) was added to 1 µl plasma and boiled for 5 min at 95°C. 50 mM ammonium bicarbonate was added and digestion was allowed to proceed overnight at 37°C using trypsin (Promega) and LysC (Wako) at 1:50 and 1:75 enzyme:substrate ratios, respectively. For OpACIN-neo samples, the digestion was quenched with 10% formic acid and the resulting peptides were cleaned-up in an automated fashion using the AssayMap Bravo platform (Agilent Technologies) with corresponding AssayMap C18 reverse-phase column. The eluate was dried and resolubilized in 1% FA to achieve a concentration of 1 µg/µl, of which 1 µL was injected. For PRADO samples, the digestion was quenched by the addition of TFA (final concentration 1%), after which the peptides were desalted

using C18 StageTips (Thermo Scientific). Samples were dried in a vacuum centrifuge and reconstituted in 2% formic acid for MS analysis.

DIA LC-MS/MS analysis

All spectra were acquired on an Orbitrap HFX mass spectrometer (Thermo Fisher Scientific) for OpACIN-neo and stage III/IV cohort samples and Orbitrap Exploris 480 Mass Spectrometer with a FAIMS-PRO interface (Thermo Fisher Scientific) for PRADO samples, operated in data-independent mode (DIA) coupled to an EASY-nLC 1200 liquid chromatography pump (Thermo Fisher Scientific) and separated on a 50 cm reversed phase column (Thermo Fisher Scientific, PepMap RSLC C18, 2 M, 100A, 75 m x 50 cm) for OpACIN-neo and stage III/IV cohort samples and on a 25 cm reversed phase column (Thermo Fisher Scientific, PepMap RSLC C18, 2 M, 100A, 75µm x 25cm) for PRADO samples.

For OpACIN-neo samples, proteome samples were eluted over a linear gradient ranging from 5-25% acetonitrile over 100 min, 25-100% acetronitrile for 5 minutes, followed by 100% acetonitrile for the final 15 minutes with a flow rate of 200 nl/min. DIA runs consisted of a MS1 scan at 60 000 resolution at m/z 200 followed by 30 sequential quadrupole isolation windows of 20 m/z for HCD MS/MS with detection of fragment ions in the OT at 30 000 resolution at m/z 200. The m/z range covered was 400–1200 and the Automatic Gain Control (AGC) was set to 1e6 for MS and 2e5 for MS/MS. The injection time was set to 100ms for MS and 'auto' for MS/MS scans.

For PRADO samples, proteome samples were eluted from the analytical column at a constant flow of 250 nl/min in a 60-min gradient, containing a 50-min linear increase from 6% to 30% solvent B, followed by a 10-min wash at 90% solvent B. FAIMS was operated in the standard resolution mode, with additional FAIMS gas flow of 3.5L/min. DIA runs consisted of a MS1 scan at 120 000 resolution at m/z 200 followed by 39 sequential quadrupole isolation windows of 15 m/z for HCD MS/MS with detection of fragment ions in the OT at 30 000 resolution at m/z 200. The m/z range covered was 400–1000 and FAIMS CV was set to -45V. The injection time was set to 45ms for MS and 'auto' for MS/MS scans.

DDA LC-MS/MS analysis for the stage III/IV cohort

A sample made of pooled representative patient serum was fractionated and fractions were injected on the same setup and gradient as the DIA experiment (as for OpACIN-neo), but the spectra were acquired in data-dependent fashion (DDA) in order to survey proteome composition in depth. The DDA data were acquired using a top-12 method where MS1 spectra had a resolving power of 60 000 at 200 m/z with an AGC target of 3e6 ions and a maximum injection time of 20 ms. MS/MS spectra were acquired with HCD

fragmentation, a normalized collision energy of 27, a 1.4-m/z-wide isolation window, a resolving power of 30 000 at 200 m/z, an AGC target of 1e5 ions and a maximum injection time of 50 ms.

Multiplex proteomics profiling

Proteins in plasma and serum samples were profiled by a multiplex assay using proximity extension assay technology (Olink Bioscience AB). A first set of serum samples of paired patient samples (n=33 patients) with stage III melanoma that progressed to stage IV melanoma were selected for investigation. To validate the findings from the first set, pre-treatment plasma samples from a second cohort of patients with stage III melanoma (OpACIN-neo study, n=86 patients) and treatment naïve patients with stage IV melanoma (n=22 patients) were selected for analysis. The Olink Immuno-Oncology panel was selected, which allows simultaneously measurement of 92 analytes by binding of oligonucleotide-labeled antibody probe pairs to their targeted protein. When in close proximity, the oligonucleotides of the probes will hybridize in a pairwise manner and can be detected and quantified using real-time polymerase chain reaction (PCR). The assay was performed at the Department of Clinical Chemistry & Hematology at the University Medical Center Utrecht. More information about the Immuno-Oncology panel, detection limits, data quantification, normalization and standardization are available on the manufacturer's website: https://www.olink.com/resources-support/document-download-center/. Analysis of the samples was performed in R (R Foundation for Statistical Computing).

Data handling and statistical analysis

For the stage III/IV cohort the proteins identified from DDA files were submitted to the Prosit tool (19) whereby artificial spectra were predicted, effectively generating an artificial spectral library. This library was in turn used to extract spectra from the DIA data using DIA-NN (20). The DIA-NN settings were as follows: "Deep learning" was enabled. The enzyme for digestion was set to trypsin with one missed cleavage tolerated and C Carbamidomethylation and M oxidation were allowed as variable modification. The precursor FDR was set to 1%. Protein grouping was done by protein names and cross-run normalization was RT-dependent. The gene-centric report was used for downstream analysis, and all runs where less than 300 proteins were identified were discarded. Technical workflow replicates were combined by taking the $\log_2$ mean value per protein. The same data handling was carried out for the OpACIN-neo study, however no spectral library was used as this was constructed directly within the DIA-NN software using the DIA raw data as basis.

For the PRADO study, the raw data reads were analyzed by DIA-NN (version 1.8) (20) without a spectral library and with "Deep learning" option enabled. The Swissprot

human database (20,375 entries, release 2022_02) fasta was added for the library-free search. The quantification strategy was set to Robust LC (high accuracy) and MBR option was enabled. The other settings were kept at the default values. The protein groups report from DIA-NN was used for downstream analysis in Perseus (version 1.6.15.0) (21). Values were Log2-transformed, after which proteins were filtered for at least 70% valid values in at least one sample group

For paired patient samples, a paired two-tailed Student's t test was used to compare the mean log_2 values. Two-tailed Student's t test and the Welch's t-test was used to compare the proteins abundance means. Additional information about quantification and statistical analyses performed are described in the corresponding figure legends. P value lower than 0.05 was regarded statistically significant. *, $P<0.05$, **, $P<0.01$, ***, $P<0.001$, ****, $P<0.0001$.

All graphic visuals and statistical analysis were performed using Prism (Graphpad Software Inc., version 9) or in R (version 4.0.4) and R studio (version 1.4.1106) using the packages survminer (version 0.4.9), ggplot2 (version 3.3.5), cutpointr (version 1.1.2), ROCit (version 2.1.1) and RColorBrewer (version1.1.-3).

Data availability statement

Data are available upon reasonable request. The mass spectrometry proteomic data have been deposited to the ProteomeXchange Consortium via the PRIDE partner repository (22) with the dataset identifier PXD04399.

Results

Previously identified CRP, SAA1, LDHB, IL-8 and IL-10 are associated with melanoma disease progression

Paired serum samples of 64 patients with stage III melanoma that progressed to stage IV melanoma were analyzed using DIA mass spectrometry (**Figure 1**, **Figure 2A**). In this paired analysis, we observed that 70 proteins (out of 445 proteins with at least an observation in the majority of patients in both stage III and IV) were significantly higher expressed when patients developed stage IV disease (**Figure 2B**). A large increase in CRP levels was observed in patients at time of stage IV disease compared to stage III disease ($P < 0.0001$; **Figure 2B**, **Figure S3A**). In addition, the previously identified markers SAA1 (14) and LDHB (12) were also increased when stage III patients progressed to stage IV melanoma (**Figure 2B**, **Figure S3B, C**).

In order to further evaluate differential expression of systemic cytokines and chemokines, we analyzed 33 paired stage III and stage IV patients for Olink proteomic assay (**Table S1**, **Figure 1**), since (usually) smaller and less abundant cytokines are difficult to detect by mass spectrometry (**Figure 2A**). This approach allowed us to evaluate 92 immuno-oncology markers. A significant higher expression of the cytokines interleukin (IL)-8 ($P = 0.0011$) and IL-10 ($P = 0.0038$) and adhesion G-protein coupled receptor G1 (ADGRG1) were observed in stage IV patients, whereas lower serum levels of Inducible T cell costimulatory ligand (ICOSLG; $P = 0.0002$) were detected (**Figure S4A**, **B**). To confirm these findings in an independent cohort, pre-treatment protein expression of 86 stage III patients were compared to 22 stage IV patients. This unpaired analysis confirmed the increased expression of IL-8 ($P = 0.0080$) and IL-10 ($P = 0.0228$; **Figure S4C**, **D**) in patients with stage IV disease. These cytokines have also previously been associated with melanoma disease progression (23, 24, 25, 26). In summary, these data show that upon disease progression increased systemic levels of CRP, SAA1, LDHB, IL-8 and IL-10 are observed upon disease progression in matched patient samples, validating previously found observations.

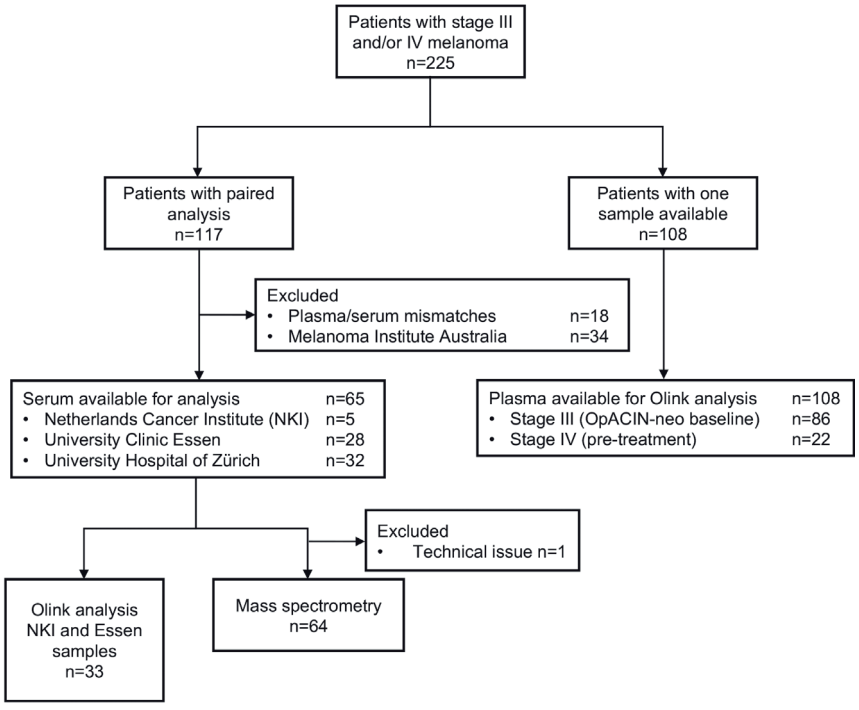

Figure 1 | Flowchart of patients with stage III and stage IV melanoma selected for serum/plasma analyses. Number of patients included for the different analysis. A total of 117 patients with paired plasma/serum samples were available at stage III disease and stage IV disease (paired analysis). Due to plasma/serum mismatch and heterogeneity between samples from European centers and Melanoma Institute Australia (MIA), the sera of 65 patients were used for analysis. Of these patients, 33 patients were analyzed by Olink and 64 patients were analyzed by Mass spectrometry (left). Plasma of 108 patients with stage III or stage IV was analyzed by Olink (right).

A

	Mass spectrometry	Olink analysis
Stage III/IV		
Paired patient samples	64	33
Unpaired patient samples *(validation cohort)*		
Stage III (samples OpACIN-neo study)		86
Stage IV		22
Neoadjuvant treatment		
OpACIN-neo study	83	
PRADO study *(validation cohort)*	49	

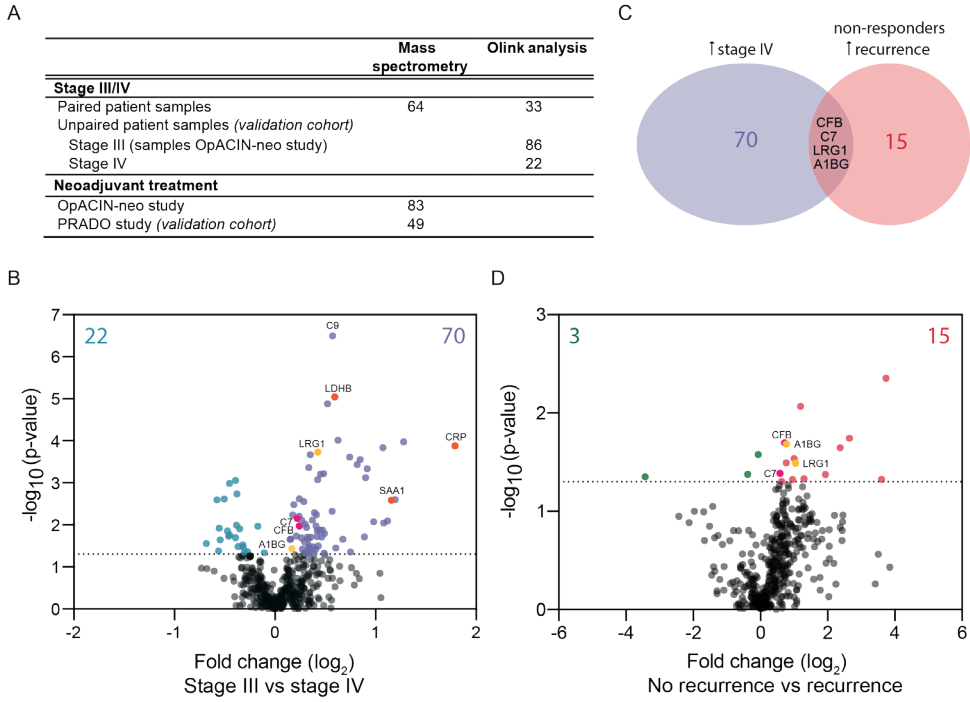

Figure 2 | Mass spectrometry analysis of protein change upon disease progression and recurrence. **(A)** Plasma and serum samples of different cohorts of melanoma patient analyzed for circulating proteins using mass spectrometry proteomic profiling and Olink analysis. **(B)** Volcano plot showing differential protein expression of serum analysis using mass spectrometry, comparing protein expression between matched patients with stage III and stage IV disease (n=64). Proteins higher expressed at stage III disease are displayed on the left, and proteins higher expressed at stage IV are displayed on the right. The protein fold change on a $\log_2$ scale is shown on the x-axis, with the significance indicated by the $-\log_{10}$ scale on the y-axis. The significance cut-off (*p*-value=0.05) is indicated with the black dotted line, showing significant increased proteins for stage III in blue and for stage IV in purple. A two-tailed paired Student's *t*-test was used to determine statistical significance between stage III and stage IV samples. **(C)** A Venn diagram for overlapping significant proteins of patients with stage IV melanoma and baseline samples of non-responding stage III patients with recurrent disease. **(D)** Volcano plot showing differential expression of plasma markers using mass spectrometry, comparing protein expression of non-responder patients of the OpACIN-neo study (n=21) with or without a recurrence. Proteins higher expressed by patients without a recurrence are displayed on the left, and proteins higher expressed by patients with a recurrence are displayed right. The protein fold change on a $\log_2$ scale is shown on the x-axis, with the significance indicated by the $-\log_{10}$ scale on the y-axis. The significance cut-off (*p*-value=0.05) is indicated with the black dotted line, showing significant increased proteins for patients without a recurrence in green and for patients with a recurrence in red. A two-tailed unpaired Welch's *t*-test was used to determine statistical significance between samples of patients with and without a recurrence.

Complement factor B (CFB), component 7 (C7) and alpha-1B glycoprotein (A1BG) expression are increased upon melanoma progression and recurrence

We next asked which markers that were increased with disease progression to stage IV disease overlapped with disease recurrence upon neoadjuvant therapy in stage III disease (**Figure 2C**). Therefore, we next analyzed baseline plasma samples of patients with stage III melanoma that were treated with dual neoadjuvant ICB (OpACIN-neo study

NCT02977052; **Table S2**) (7, 18). Patients who achieved a pathological response seldom relapsed (2-year relapse-free survival (RFS) 97%), whereas those without a pathologic response had a poor RFS (2-year 36%) (18). Therefore, it is particularly important to investigate predicting biomarkers for recurrent disease within the non-responding patient cohort to identify patients that might require intensified therapies. Accordingly, we compared baseline plasma of patients without a pathological response that had a recurrence to those without a recurrence (n=21; **Figure 2C-D**, **Figure S1**).

Comparing significant increased proteins of patients with stage IV melanoma that were shared with significantly increased proteins in baseline samples of non-responding stage III patients with recurrent disease revealed an overlap for leucine-rich alpha-2-glycoprotein 1 (LRG1), alpha-1B glycoprotein (A1BG) and complement factor/component (**Figure 2B-D**). The complement component (C7), complement factor B (CFB) and A1BG showed a significant increased expression in patients with stage IV melanoma ($P = 0.0070$, $P = 0.0107$, $P = 0.0371$, respectively) and non-responding patients with a recurrence ($P = 0.0302$, $P = 0.0400$, $P = 0.0208$, respectively). However, no significant association was observed with pathological response to neoadjuvant ICB for these markers (**Figure S5A-C**).

Next, we evaluated whether certain expression levels of C7, CFB and A1BG could predict event-free survival (EFS) for patients without a response upon neoadjuvant ipilimumab and nivolumab. Optimal cutoffs for these markers were defined based on summary receiver operating characteristic (sROC) curves, using the complete OpACIN-neo patient cohort (responding and non-responding patients, n=82 for C7; n=83 for CFB and A1BG). We identified 23.2738, 26.212 and 27.2107, as the optimal cut off for protein abundance of C7, CFB and A1BG, respectively, resulting in an area under the sROC curve (AUC) of 0.621, 0.628 and 0.698, respectively. Patients with a high versus low C7 expression showed no significant difference in EFS ($P = 0.062$; **Figure S5D**), while patients with either high CFB or high A1BG expression had a significantly lower EFS following neoadjuvant ICB treatment ($P = 0.016$, $P = 0.0064$; **Figure S5E, F**).

To validate the prognostic impact of systemic expression of CFB and A1BG, baseline plasma samples of a second cohort of patients (n=49) treated with neoadjuvant ipilimumab and nivolumab (8) were analyzed (**Table S3**, **Figure S2**). The samples were analyzed on a different mass spectrometer, and therefore a new optimal cut-off was calculated. The AUC to discriminate between patients with and without a recurrence for CFB and A1BG was lower in the PRADO cohort compared to the OpACIN-neo cohort (CFB: 0.572, A1BG: 0.609). Moreover, no significant difference for EFS was observed for non-responding patients with either a high CFB or A1BG compared to a low CFB or A1BG expression, respectively (**Figure S5G-H**). Thus, these markers could not be validated

in an independent cohort, and therefore it remains uncertain whether systemic CFB and A1BG have prognostic potential for disease recurrence in non-responding stage III melanoma patients treated with neoadjuvant ICB.

LRG1 expression is associated with melanoma progression and recurrence

The analysis of significantly increased proteins associated with both disease progression and disease recurrence also identified LRG1 as an overlapping marker (**Figure 2B, D**). A significantly higher expression of LRG1 was observed in serum of stage IV disease patients compared to the matching stage III samples (P = 0.0002; **Figure 3A**). For non-responding patients of the OpACIN-neo cohort, there was a significantly higher expression of LRG1 in baseline samples for patients with a recurrence in comparison to patients without a recurrence (P = 0.0156; **Figure 3B**). This significant difference was only significant at baseline, and no significant difference was found after neo-adjuvant ICB at week 6 (moment of surgery; **Figure 3C**). When evaluating the prognostic value of LRG1 for pathological response, there was no significant difference between responding and non-responding patients upon neoadjuvant ICB treatment (**Figure 3D**).

Subsequently, we assessed whether we were able to predict at baseline if OpACIN-neo patients were more likely to have a recurrence based on their LRG1 expression, identifying 24.5504 as the optimal cut-off for LRG1 based on the sROC curve. The AUC was higher for non-responding patients (0.780) compared to the whole patient cohort (0.598; **Figure 3E**). Based on this cut-off, we could discriminate patients with a high and low baseline LRG1 protein expression. When comparing both groups in the total cohort of all responding and non-responding patients, no significant difference in EFS was found (P = 0.084; **Figure 3F**). However, when patients with a high versus low baseline LRG1 expression were compared in the subgroup of patients that had no response upon neoadjuvant ICB treatment, a significantly lower EFS was observed in patients with a high LRG1 expression (P = 0.014; **Figure 3G**). After a median follow-up of 47 months, 5 patients with high LRG1 expression have died, while none of the patients with low LRG1 expression has died. This difference was not (yet) significant (P = 0.11; **Figure 3H**).

As neutrophils are among the cell types that secrete LRG1 (27), we analyzed whether baseline neutrophil count was associated with systemic LRG1 expression. No correlation between systemic LRG1 expression and neutrophil count was observed (**Figure S6A**). Furthermore, high neutrophil count and high neutrophil-to-lymphocyte ratio (NLR), which has been associated with poor prognosis (28), was not significantly associated with recurrence in non-responding patients (**Figure S6B, C**).

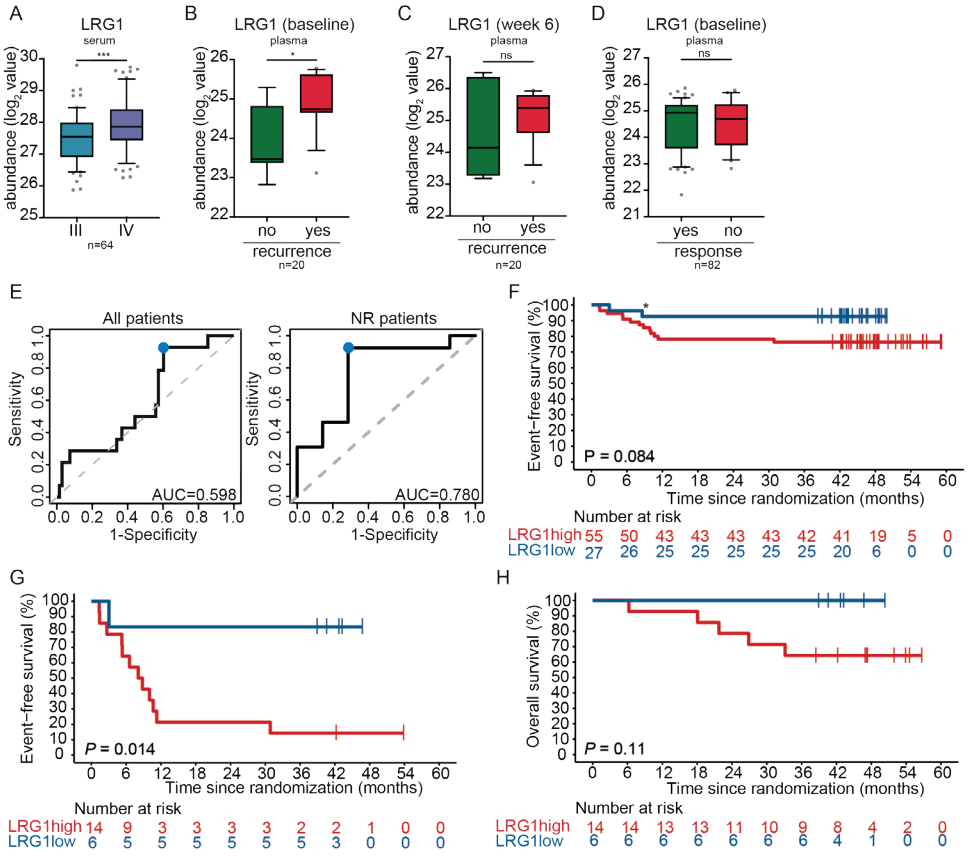

Figure 3 | LRG1 expression is associated with melanoma progression and recurrence. **(A-D)** Normalized protein expression (log_2) values of LRG1, measured by mass spectrometry for **(A)** matched stage III and IV patients (n=64) **(B)** non-responsive patients at baseline of the OpACIN-neo study (n=20) and **(C)** at week 6 after neoadjuvant ICB treatment of the OpACIN-neo study (n=20) and **(D)** all patients at baseline of the OpACIN-neo study (n=82). A two-tailed paired Student's *t*-test was used to determine statistical significance between stage III and stage IV samples. A two-tailed unpaired Student's *t*-test was used to compare patients with and without a recurrence or response of the OpACIN-neo study. **(E)** Summary receiver operating characteristic (sROC) curves to define the optimal cut-off (marked by the blue dot) for all patients (left) and non-responding patients (right) of the OpACIN-neo study for baseline LRG1 expression. The area under the sROC curve (AUC) for all patients was 0.598 and for non-responder patients 0.780, with an optimal cut-off of 24.5504. **(F-G)** A Kaplan Meier curve showing event-free survival (EFS) for **(F)** all patients and **(G)** non-responder patients of the OpACIN-neo study with either a high (red) or low (blue) expression of LRG1. The asterisk denotes a patient (in LRG1 low group) who died due to irAEs. **(H)** A Kaplan Meier curve showing overall survival (OS) for non-responder patients of the OpACIN-neo study with either a high (red) or low (blue) expression of LRG1. *P* value was calculated using the log-rank test (two-sided) and significance is indicated. *, $P<0.05$, ***, $P<0.001$

LRG1 is associated with melanoma recurrence in a second independent cohort of stage III melanoma patients treated with neoadjuvant ipilimumab + nivolumab

To confirm the prognostic potential of LRG1, we analyzed pre-treatment plasma samples of a second independent cohort (PRADO) of patients who were also treated with neoadjuvant ipilimumab and nivolumab (**Table S3**, **Figure S2**) (8). In this cohort, we

determined whether we were also able to identify patients who had a recurrence based on their LRG1 expression, using the sROC curves to define the optimal cut-off. A different cut-off was used, since this cohort was analyzed on a different mass spectrometer. Using this strategy, a cut-off for LRG1 of 24.9485 was determined, corresponding to an AUC of 0.588 for all patients and 0.714 for patients not responding to treatment (**Figure 4A**). Consequently, patients were divided into LRG1 high and LRG1 low baseline protein expression. Patients with a high LRG1 expression had a significantly lower 2-year EFS compared to patients with a low LRG1 expression ($P = 0.0037$; **Figure 4B**). This was even more pronounced in the non-responding patients, where all patients with a high LRG1 expression experienced a disease recurrence within 6 months after start treatment versus only 14% in the LRG1 low group ($P = 0.0021$; **Figure 4C**).

In summary, these data validate in two independent cohorts that pre-treatment systemic LRG1 expression is a prognostic marker for disease recurrence after neoadjuvant treatment with ICB, especially in patients who do not respond to neoadjuvant ICB.

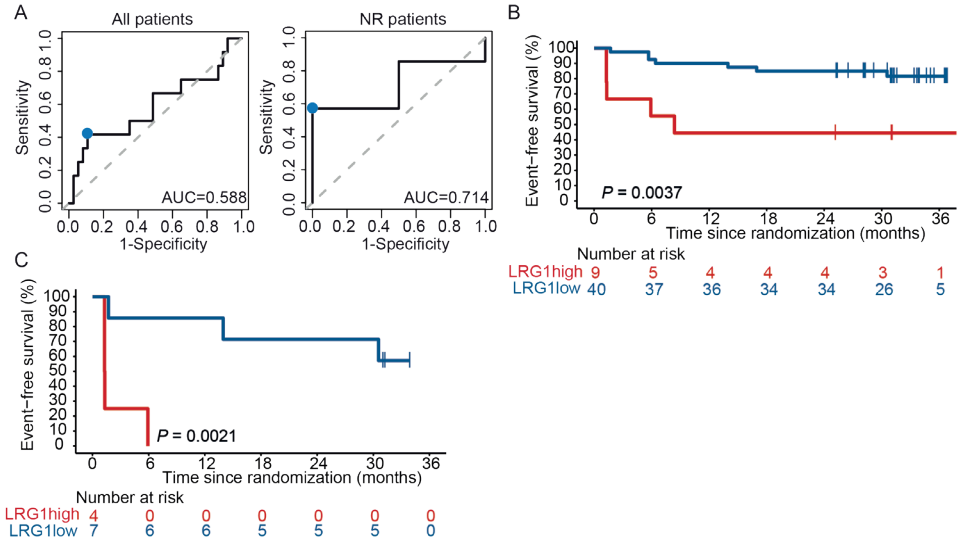

Figure 4 | LRG1 expression is associated with melanoma recurrence in a second independent cohort. **(A)** Summary receiver operating characteristic (sROC) curves to define the optimal cut-off (marked by the blue dot) for all patients (left) and non-responding patients (right) of the PRADO study for baseline LRG1 expression in patient plasma. The area under the sROC curve (AUC) for all patients was 0.588 and for non-responder patients 0.714, with an optimal cut-off of 24.9485. **(B-C)** A Kaplan Meier curve showing event-free survival (EFS) for **(B)** all patients (n=49) and **(C)** non-responder patients (n=11) of the PRADO study with either a high (red) or low (blue) expression LRG1. *P* value was calculated using the log-rank test (two-sided) and significance is indicated.

High LRG1 expression is associated with distant metastasis in patients that do not respond to neoadjuvant ipilimumab and nivolumab

Patients without a pathological response after neoadjuvant ICB therapy were more likely to develop a recurrence compared to patients with a pathological response (8, 18, 29). These recurrences were either at local or distant sites. Next, we assessed whether LRG1 was associated with the site of recurrence. We observed that all non-responder patients that developed a distant metastasis showed higher baseline systemic LRG1 protein expression. In the OpACIN-neo study, a significantly higher expression of LRG1 was found at baseline for patients that had a distant recurrence compared to patients without recurrent disease ($P = 0.0159$), whereas no significant difference was found compared to local recurrence (**Figure 5A**). Comparing LRG1 expression of patients that developed a distant recurrence to patients without a recurrence in PRADO, only a trend for increased levels of LRG1 was found ($P = 0.0618$; **Figure 5B**). This analysis showed that patients that developed a distant recurrence have a higher pre-treatment expression of LRG1 compared to patients without a recurrence or those that recurred at a local site only.

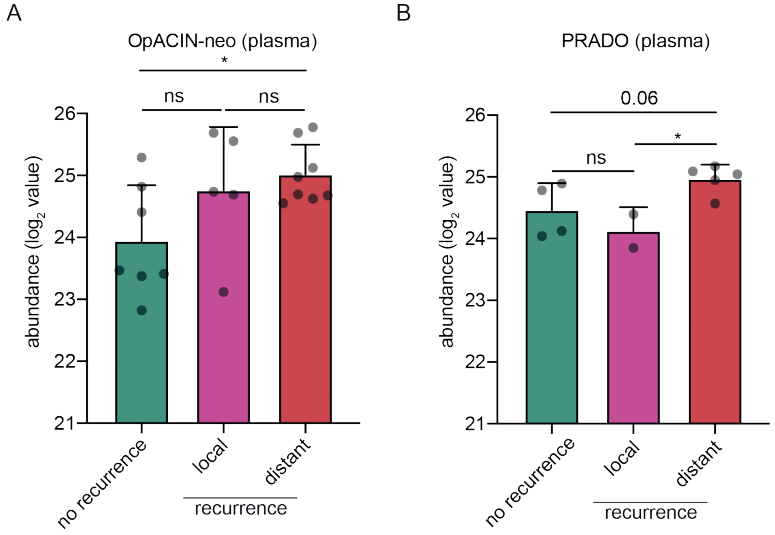

Figure 5 | High LRG1 expression is associated with distant metastasis in patients that do not respond to neoadjuvant ipilimumab and nivolumab. LRG1 expression measured in patient plasma by mass spectrometry for patients without a response upon neoadjuvant ICB of the **(A)** OpACIN-neo study (n=20) and **(B)** PRADO study (n=11). Comparing patients without a recurrence (green), patients with a local recurrence (pink) and patients with a distant recurrence (red). A two-tailed unpaired Student's *t*-test for comparing patient groups. *, $P<0.05$

Discussion

Treatment of advanced-stage melanoma patients with ICB has demonstrated unprecedented success (30, 31). In the setting of neoadjuvant treatment even higher

response rates are achieved (4, 7, 8, 32, 33). In our cohort (OpACIN-neo and PRADO study NCT02977052), high pathological response rates, with durable cancer control were observed with 2-year RFS of 84-85%. Still, a subset of patients did not respond (24-28% of patients) and these patients were much more likely to develop a recurrence of melanoma. Additional adjuvant treatment of non-responding patients after neoadjuvant ICB increased the 2-year RFS from 36% to 71% (8, 18), highlighting that this patient group could benefit from additional therapies. Hence, it is particularly important to identify patients without a pathologic response after neoadjuvant ICB who are at risk for disease recurrence and therefore could benefit from adjuvant therapy. Based on the observation that systemic immune response is required for immunotherapeutic efficacy (9, 34), we postulated that patients with disease progression and recurrence have a higher degree of systemic immune suppression, hampering an effective immune response. Accordingly, we analyzed the systemic protein expression of melanoma patients with mass-spectrometry based protein profiling and Olink analysis using an unbiased approach.

In our screen we confirmed previously identified markers CRP, SAA1, LDHB, IL-8 and IL-10 (12, 13, 14, 23, 24, 25) to be associated with disease progression, making our patient cohort for disease progression a representative cohort. Of note, IL-8 and IL-10 were not detected by mass spectrometry, since most cytokines are difficult to identify by mass spectrometry, which prompted us to conduct Olink analysis. The cohort included matched patients that progressed from stage III to stage IV melanoma, making this a unique patient group.

Our study also has some limitations that need to be considered. All the analysis were performed without a correction for multiple testing. In addition, all patients progressed to stage IV disease, thus there is a selection bias for patients with worse prognosis. Another limitation of our cohort is the low number of patients, especially the number of non-responding patients upon neoadjuvant therapy in OpACIN-neo and PRADO cohort is small. Moreover, not all markers were validated in the different independent cohorts and different cut-off for these markers were used, since the patient samples of the OpACIN-neo and PRADO cohort were measured on different mass spectrometers. Furthermore, non-responding patients in the PRADO cohort received adjuvant therapy, while this was not applied in the OpACIN-neo cohort. Future studies that use a uniform cut-off and includes statistical adjustment of the data for multiple testing for a higher number of patients will strengthen the findings of this study. Nevertheless, we consider these homogeneous cohorts as the best available to identify circulating proteins that are potentially associated with systemic immune suppression. In particular, comparing the results from these patients with progressive disease to two independent cohorts of stage III melanoma patients treated with neoadjuvant treatment, with only differences

in dose levels in the treatment regimes, allowed us to more confidently identify markers associated with disease progression as well as disease recurrence.

In addition, when comparing proteins between stage IV patients with progressive disease and initial stage III patients with recurrent local or distant disease, increased LRG1 expression was found in both patient cohorts. LRG1 is a secreted glycoprotein that is constitutively synthesized by hepatocytes and neutrophils under physiological conditions (27). Following various inflammatory stimuli, including IL-1b, IL-6, IL-10, IL-17, IL-22, IL-33, tumor necrosis factor alpha (TNF-a) and transforming growth factor beta (TGF-b), secretion of LRG1 is increased predominantly by hepatocytes, neutrophils and endothelial cells and can be detected systemically and/or at the local tissue level (35). Tumor and stromal cells within the tumor microenvironment (TME) can also be a source of LRG1, and circulating levels of LRG1 were previously shown to be correlated with disease progression, disease burden, and poor prognosis in different cancer types (e.g. gastrointestinal, lung, pancreatic, prostate cancer) (36, 37, 38, 39, 40, 41, 42), but not melanoma.

Here, we show for the first time that systemic LRG1 expression is also increased during melanoma disease progression. Moreover, pre-treatment elevated circulating levels of LRG1 were also associated with poor patient outcome after neoadjuvant ICB therapy. These data further support the relevance of LRG1 in cancer (progression).

LRG1 has previously been described to promote cancer pathogenesis, either directly or indirectly. LRG1 contributes directly to tumor cell viability and proliferation (43, 44), promoting epithelial-to-mesenchymal transition (EMT) (35) and promoting dysfunctional angiogenesis (45). It also acts indirectly by modifying the TGF-b signaling pathway (46) and enhancing expression of pro-angiogenic factors (vascular endothelial growth factor A; VEGFA and Angiopoietin-1) (47, 48). TGF-b signaling has been shown to directly inhibit anti-tumor immune responses (49).

This is in line with our observation that LRG1 is associated with disease recurrence, and non-responding patients had a particularly poor prognosis when increased LRG1 expression was observed. Furthermore, the highest expression of LRG1 was found in patients that developed a distant metastasis. Our findings support previous findings that LRG1 enhances metastatic dissemination and contributes to the metastatic niche (35). However, further investigations are required to determine whether LRG1 is indeed mechanistically contributing to metastasis formation in melanoma patients.

Factors from the complement system, CFB and C7, and A1BG were also found to be significantly increased in both patients with progressive and recurrent disease. However,

in our independent cohort, these findings could not be confirmed. A1BG, a member of the immunoglobulin superfamily, with unknown function (50), has been described to be elevated in pancreatic ductal adenocarcinoma (51) and urinary samples from bladder cancer patients (52). The complement system plays a major, but complex role in cancer due to opposing effects, which is dependent of the context (site activation, composition TME, tumor cell sensitivity to complement) (53). Although previous studies support a negative role for CFB (54) in squamous cell carcinoma mouse models, and C7 in patients with glioma (55), the role of these complement factors in melanoma disease recurrence needs to be further elucidated.

Biomarkers that are associated with disease recurrence and progression could serve as therapeutic targets, especially when these markers are causal to immune suppressive effects. Since IL-8 was previously shown to be expressed in higher levels in patients that progressed from II to stage III melanoma (23), it is a poor prognostic marker in stage IV melanoma, and a decrease in levels from baseline are correlated with response to anti-PD-1 treatment (25), an anti-IL-8 antibody (HuMax-IL8, BMS-986253) has been developed. In a study (NCT03400332) testing nivolumab + anti-IL-8 therapy in patients with increased IL-8 serum levels showed dose-proportional pharmacokinetics and reduction in serum IL-8 levels, resulting in partial responses (56).

Considering our data that shows increased levels of LRG1 to be associated with disease progression and recurrence, novel treatment strategies could explore the therapeutic potential of targeting LRG1. Currently, anti-LRG1 treatment has only been tested in mouse models, and showed reduced tumor growth and synergistic effect with anti-PD-1 (45, 57). Additionally, anti-LRG1 improved vascular function, and therefore, it is hypothesized that this vascular normalization leads to improved delivery of immunotherapies (or other therapies) (45, 58). Moreover, it has been shown that systemic immune changes can be reversed, revealing the plasticity of the systemic immune state (34). Although these preclinical results are promising, further studies are needed to assess the clinical therapeutic utility of anti-LRG1 therapy. In addition, it would be of interest to assess whether LRG1 levels are elevated in non-responding patients after surgery when adjuvant treatment decisions are made.

In conclusion, we identified LRG1 as a potential biomarker for recurrence in patients treated with neoadjuvant ICB, which could serve as marker for intensified adjuvant treatment and follow-up. Given the cumulating data on LRG-1 and cancer progression, further supported by mouse data indicating improved tumor control upon LRG-1 inhibition in combination with ICB, we envision that LRG1 could become, not only a biomarker, but also a possible target for combination therapy with ICB for patients with an unfavorable response after treatment with neoadjuvant immunotherapy.

Acknowledgement

We thank all members of the Blank, Altelaar and Peeper laboratory for valuable discussion. We would like to acknowledge the NKI-AVL Core Facility Molecular Pathology & Biobanking (CFMPB) for supplying NKI-AVL Biobank material and/or lab support. This work has been supported by EPIC-XS, project number 823839, funded by the Horizon 2020 programme of the European Union and the NWO funded Netherlands Proteomics Centre through the National Road Map for Large-scale Infrastructures program X-Omics, Project 184.034.019.

Author Contribution

E.P. Hoefsmit: Conceptualization, resources, data curation, formal analysis, validation, investigation, visualization, methodology, writing-original draft, project administration. F. Völlmy: Conceptualization, resources, data curation, formal analysis, validation, investigation, visualization, methodology, writing-original draft, project administration, writing-review and editing. E.A. Rozeman: Conceptualization, resources, data curation, formal analysis, validation, investigation, writing-original draft, project administration, writing-review and editing. I.L.M. Reijers: Resources, data curation, project administration, writing-review and editing. J.M. Versluis: Resources, data curation, writing-review and editing. L. Hoekman: Data curation, formal analysis, validation, writing-review and editing. A.C.J. van Akkooi: Resources, data curation, writing-review and editing. G.V. Long: Resources, data curation, writing-review and editing. D. Schadendorf: Resources, data curation, writing-review and editing. R. Dummer: Resources, data curation, writing-review and editing. M. Altelaar: Conceptualization, resources, data curation, supervision, funding acquisition, writing-review and editing. C.U. Blank: Conceptualization, resources, data curation, supervision, funding acquisition, writing-original draft, writing-review and editing.

Financial support

This work was financially supported by Bristol-Myers Squibb (BMS) via II-ON project OT123-291

COI

A.C.J. van Akkooi reports grants and personal fees from Amgen, Merck-Pfizer; personal fees from Bristol-Myers Squibb, MSD-Merck, Novartis, Pierre Fabre, Sirius Medical, 4SC, and Sanofi outside the submitted work. G.V. Long reports personal fees from Agenus Inc, Amgen Inc, Array Biopharma, Boehringer Ingelheim, BMS, Evaxion Biotech, Hexal

AG, Highlight Therapeutics, Innovent Biologics, MSD, Novartis Pharma, OncoSec, PHMR, Pierre Fabre, Provectus, Qbiotics Group, and Regeneron outside the submitted work. D. Schadendorf reports grants from Roche, BMS, Novartis, Amgen, MSD and personal fees from Novartis, MSD, BMS, Ultimovacs, InFlarX, Haystack, Innovent, Immatics, Nektar, AstraZeneca, Daiichi Sanyo, Labcorp, BioAlta, Immunocore, SunPharma,Pierre Fabre, Neracare, Sanofi outside the submitted work. C.U. Blank reports grants from BMS, Novartis, NanoString, 4SC; personal fees from advisory role: BMS, MSD, Roche, Novartis, GSK, AZ, Pfizer, Lilly, GenMab, Pierre Fabre, Third Rock Ventures; and other from Stockownership: co-founder Immagene BV and Signature Oncology outside the submitted work; in addition, C.U. Blank has a patent to Patents (incl. submitted): WO 2021/177822 A1, N2027907, P091040NL2 pending. No disclosures were reported by the other authors.

References

1. Hodi FS, O'Day SJ, McDermott DF, Weber RW, Sosman JA, Haanen JB, et al. Improved survival with ipilimumab in patients with metastatic melanoma. New England Journal of Medicine. 2010;363(8):711-23.
2. Schadendorf D, Hodi FS, Robert C, Weber JS, Margolin K, Hamid O, et al. Pooled analysis of long-term survival data from phase II and phase III trials of ipilimumab in unresectable or metastatic melanoma. Journal of clinical oncology. 2015;33(17):1889.
3. Larkin J, Chiarion-Sileni V, Gonzalez R, Grob JJ, Cowey CL, Lao CD, et al. Combined nivolumab and ipilimumab or monotherapy in untreated melanoma. New England journal of medicine. 2015;373(1):23-34.
4. Larkin J, Chiarion-Sileni V, Gonzalez R, Grob J-J, Rutkowski P, Lao CD, et al. Five-year survival with combined nivolumab and ipilimumab in advanced melanoma. New England Journal of Medicine. 2019;381(16):1535-46.
5. Wolchok JD, Chiarion-Sileni V, Gonzalez R, Rutkowski P, Grob J-J, Cowey CL, et al. Overall survival with combined nivolumab and ipilimumab in advanced melanoma. New England Journal of Medicine. 2017;377(14):1345-56.
6. Blank CU, Rozeman EA, Fanchi LF, Sikorska K, van de Wiel B, Kvistborg P, et al. Neoadjuvant versus adjuvant ipilimumab plus nivolumab in macroscopic stage III melanoma. Nature medicine. 2018;24(11):1655-61.
7. Rozeman EA, Menzies AM, van Akkooi AC, Adhikari C, Bierman C, van de Wiel BA, et al. Identification of the optimal combination dosing schedule of neoadjuvant ipilimumab plus nivolumab in macroscopic stage III melanoma (OpACIN-neo): a multicentre, phase 2, randomised, controlled trial. The Lancet Oncology. 2019;20(7):948-60.
8. Reijers ILM, Menzies AM, van Akkooi ACJ, Versluis JM, van den Heuvel NMJ, Saw RPM, et al. Personalized response-directed surgery and adjuvant therapy after neoadjuvant ipilimumab and nivolumab in high-risk stage III melanoma: the PRADO trial. Nat Med. 2022;28(6):1178-88.
9. Spitzer MH, Carmi Y, Reticker-Flynn NE, Kwek SS, Madhireddy D, Martins MM, et al. Systemic Immunity Is Required for Effective Cancer Immunotherapy. Cell. 2017;168(3):487-502.e15.
10. Lui V, Karpuchas J, Dent P, McCulloch P, Blajchman M. Cellular immunocompetence in melanoma: effect of extent of disease and immunotherapy. British Journal of Cancer. 1975;32(3):323-30.
11. Hauschild A, Engel G, Brenner W, Gläser R, Mönig H, Henze E, et al. S100B protein detection in serum is a significant prognostic factor in metastatic melanoma. Oncology. 1999;56(4):338-44.
12. Utikal J, Schadendorf D, Ugurel S. Serologic and immunohistochemical prognostic biomarkers of cutaneous malignancies. Archives of Dermatological Research. 2007;298(10):469-77.
13. Fang S, Wang Y, Sui D, Liu H, Ross MI, Gershenwald JE, et al. C-reactive protein as a marker of melanoma progression. J Clin Oncol. 2015;33(12):1389-96.
14. Findeisen P, Zapatka M, Peccerella T, Matzk H, Neumaier M, Schadendorf D, et al. Serum amyloid A as a prognostic marker in melanoma identified by proteomic profiling. J Clin Oncol. 2009;27(13):2199-208.
15. Wagner NB, Forschner A, Leiter U, Garbe C, Eigentler TK. S100B and LDH as early prognostic markers for response and overall survival in melanoma patients treated with anti-PD-1 or combined anti-PD-1 plus anti-CTLA-4 antibodies. Br J Cancer. 2018;119(3):339-46.
16. Wu C, Duan J, Liu T, Smith RD, Qian W-J. Contributions of immunoaffinity chromatography to deep proteome profiling of human biofluids. Journal of Chromatography B. 2016;1021:57-68.
17. Altelaar A, Munoz J, Heck AJ. Next-generation proteomics: towards an integrative view of proteome dynamics. Nature Reviews Genetics. 2013;14(1):35-48.
18. Rozeman E, Hoefsmit E, Reijers I, Saw R, Versluis J, Krijgsman O, et al. Survival and biomarker analyses from the OpACIN-neo and OpACIN neoadjuvant immunotherapy trials in stage III melanoma. Nature Medicine. 2021:1-8.
19. Gessulat S, Schmidt T, Zolg DP, Samaras P, Schnatbaum K, Zerweck J, et al. Prosit: proteome-wide prediction of peptide tandem mass spectra by deep learning. Nat Methods. 2019;16(6):509-18.
20. Demichev V, Messner CB, Vernardis SI, Lilley KS, Ralser M. DIA-NN: neural networks and interference correction enable deep proteome coverage in high throughput. Nat Methods. 2020;17(1):41-4.
21. Tyanova S, Temu T, Sinitcyn P, Carlson A, Hein MY, Geiger T, et al. The Perseus computational platform for comprehensive analysis of (prote)omics data. Nature Methods. 2016;13(9):731-40.
22. Vizcaíno JA, Csordas A, Del-Toro N, Dianes JA, Griss J, Lavidas I, et al. 2016 update of the PRIDE database and its related tools. Nucleic acids research. 2016;44(D1):D447-D56.

23. Ugurel S, Rappl G, Tilgen W, Reinhold U. Increased serum concentration of angiogenic factors in malignant melanoma patients correlates with tumor progression and survival. J Clin Oncol. 2001;19(2):577-83.
24. Dummer W, Becker JC, Schwaaf A, Leverkus M, Moll T, Bröcker EB. Elevated serum levels of interleukin-10 in patients with metastatic malignant melanoma. Melanoma Res. 1995;5(1):67-8.
25. Sanmamed M, Perez-Gracia J, Schalper K, Fusco J, Gonzalez A, Rodriguez-Ruiz M, et al. Changes in serum interleukin-8 (IL-8) levels reflect and predict response to anti-PD-1 treatment in melanoma and non-small-cell lung cancer patients. Annals of Oncology. 2017;28(8):1988-95.
26. Wilmott JS, Haydu LE, Menzies AM, Lum T, Hyman J, Thompson JF, et al. Dynamics of chemokine, cytokine, and growth factor serum levels in BRAF-mutant melanoma patients during BRAF inhibitor treatment. The Journal of Immunology. 2014;192(5):2505-13.
27. O'Donnell LC, Druhan LJ, Avalos BR. Molecular characterization and expression analysis of leucine-rich α2-glycoprotein, a novel marker of granulocytic differentiation. Journal of leukocyte biology. 2002;72(3):478-85.
28. Capone M, Giannarelli D, Mallardo D, Madonna G, Festino L, Grimaldi AM, et al. Baseline neutrophil-to-lymphocyte ratio (NLR) and derived NLR could predict overall survival in patients with advanced melanoma treated with nivolumab. Journal for ImmunoTherapy of Cancer. 2018;6(1):74.
29. Menzies AM, Amaria RN, Rozeman EA, Huang AC, Tetzlaff MT, van de Wiel BA, et al. Pathological response and survival with neoadjuvant therapy in melanoma: a pooled analysis from the International Neoadjuvant Melanoma Consortium (INMC). Nature Medicine. 2021;27(2):301-9.
30. Robert C, Ribas A, Schachter J, Arance A, Grob JJ, Mortier L, et al. Pembrolizumab versus ipilimumab in advanced melanoma (KEYNOTE-006): post-hoc 5-year results from an open-label, multicentre, randomised, controlled, phase 3 study. Lancet Oncol. 2019;20(9):1239-51.
31. Hodi FS, -Sileni VC, Lewis KD, Grob J-J, Rutkowski P, Lao CD, et al. Long-term survival in advanced melanoma for patients treated with nivolumab plus ipilimumab in CheckMate 067. Journal of Clinical Oncology. 2022;40(16_suppl):9522-.
32. Robert C, Ribas A, Schachter J, Arance A, Grob J-J, Mortier L, et al. Pembrolizumab versus ipilimumab in advanced melanoma (KEYNOTE-006): post-hoc 5-year results from an open-label, multicentre, randomised, controlled, phase 3 study. The Lancet Oncology. 2019;20(9):1239-51.
33. Patel SP, Othus M, Moon J, Tetzlaff M, Buchbinder EI, Sondak VK, et al. S1801: A randomized trial of adjuvant versus neoadjuvant pembrolizumab for melanoma. Wolters Kluwer Health; 2021.
34. Allen BM, Hiam KJ, Burnett CE, Venida A, DeBarge R, Tenvooren I, et al. Systemic dysfunction and plasticity of the immune macroenvironment in cancer models. Nature Medicine. 2020;26(7):1125-34.
35. Camilli C, Hoeh AE, De Rossi G, Moss SE, Greenwood J. LRG1: an emerging player in disease pathogenesis. Journal of Biomedical Science. 2022;29(1):6.
36. Zhang Q, Huang R, Tang Q, Yu Y, Huang Q, Chen Y, et al. Leucine-rich alpha-2-glycoprotein-1 is upregulated in colorectal cancer and is a tumor promoter. OncoTargets and therapy. 2018;11:2745.
37. Surinova S, Choi M, Tao S, Schüffler PJ, Chang CY, Clough T, et al. Prediction of colorectal cancer diagnosis based on circulating plasma proteins. EMBO molecular medicine. 2015;7(9):1166-78.
38. Nambu M, Masuda T, Ito S, Kato K, Kojima T, Daiko H, et al. Leucine-rich alpha-2-glycoprotein 1 in serum is a possible biomarker to predict response to preoperative chemoradiotherapy for esophageal cancer. Biological and Pharmaceutical Bulletin. 2019;42(10):1766-71.
39. Yamamoto M, Takahashi T, Serada S, Sugase T, Tanaka K, Miyazaki Y, et al. Overexpression of leucine-rich α2-glycoprotein-1 is a prognostic marker and enhances tumor migration in gastric cancer. Cancer Science. 2017;108(10):2052-60.
40. Guergova-Kuras M, Kurucz I, Hempel W, Tardieu N, Kadas J, Malderez-Bloes C, et al. Discovery of lung cancer biomarkers by profiling the plasma proteome with monoclonal antibody libraries. Molecular & Cellular Proteomics. 2011;10(12).
41. Capello M, Bantis LE, Scelo G, Zhao Y, Li P, Dhillon DS, et al. Sequential validation of blood-based protein biomarker candidates for early-stage pancreatic cancer. JNCI: Journal of the National Cancer Institute. 2017;109(4).
42. Guldvik IJ, Zuber V, Braadland PR, Grytli HH, Ramberg H, Lilleby W, et al. Identification and Validation of Leucine-rich α-2-glycoprotein 1 as a Noninvasive Biomarker for Improved Precision in Prostate Cancer Risk Stratification. European urology open science. 2020;21:51-60.

43. Xie Z-B, Zhang Y-F, Jin C, Mao Y-S, Fu D-L. LRG-1 promotes pancreatic cancer growth and metastasis via modulation of the EGFR/p38 signaling. Journal of Experimental & Clinical Cancer Research. 2019;38(1):1-12.
44. Zhong D, Zhao S, He G, Li J, Lang Y, Ye W, et al. Stable knockdown of LRG1 by RNA interference inhibits growth and promotes apoptosis of glioblastoma cells in vitro and in vivo. Tumor Biology. 2015;36(6):4271-8.
45. O'Connor MN, Kallenberg DM, Camilli C, Pilotti C, Dritsoula A, Jackstadt R, et al. LRG1 destabilizes tumor vessels and restricts immunotherapeutic potency. Med. 2021;2(11):1231-52. e10.
46. Wang X, Abraham S, McKenzie JA, Jeffs N, Swire M, Tripathi VB, et al. LRG1 promotes angiogenesis by modulating endothelial TGF-β signalling. Nature. 2013;499(7458):306-11.
47. Zhang J, Zhu L, Fang J, Ge Z, Li X. LRG1 modulates epithelial-mesenchymal transition and angiogenesis in colorectal cancer via HIF-1α activation. Journal of Experimental & Clinical Cancer Research. 2016;35(1):29.
48. Li Z, Zeng C, Nong Q, Long F, Liu J, Mu Z, et al. Exosomal Leucine-Rich-Alpha2-Glycoprotein 1 Derived from Non-Small-Cell Lung Cancer Cells Promotes Angiogenesis via TGF-β Signal Pathway. Molecular Therapy - Oncolytics. 2019;14:313-22.
49. Batlle E, Massagué J. Transforming Growth Factor-β Signaling in Immunity and Cancer. Immunity. 2019;50(4):924-40.
50. Ishioka N, Takahashi N, Putnam FW. Amino acid sequence of human plasma alpha 1B-glycoprotein: homology to the immunoglobulin supergene family. Proc Natl Acad Sci U S A. 1986;83(8):2363-7.
51. Tian M, Cui Y-Z, Song G-H, Zong M-J, Zhou X-Y, Chen Y, et al. Proteomic analysis identifies MMP-9, DJ-1 and A1BG as overexpressed proteins in pancreatic juice from pancreatic ductal adenocarcinoma patients. BMC Cancer. 2008;8(1):241.
52. Kreunin P, Zhao J, Rosser C, Urquidi V, Lubman DM, Goodison S. Bladder cancer associated glycoprotein signatures revealed by urinary proteomic profiling. Journal of proteome research. 2007;6(7):2631-9.
53. Roumenina LT, Daugan MV, Petitprez F, Sautès-Fridman C, Fridman WH. Context-dependent roles of complement in cancer. Nature Reviews Cancer. 2019;19(12):698-715.
54. Riihilä P, Nissinen L, Farshchian M, Kallajoki M, Kivisaari A, Meri S, et al. Complement component C3 and complement factor B promote growth of cutaneous squamous cell carcinoma. The American Journal of Pathology. 2017;187(5):1186-97.
55. Bacolod MD, Talukdar S, Emdad L, Das SK, Sarkar D, Wang XY, et al. Immune infiltration, glioma stratification, and therapeutic implications. Transl Cancer Res. 2016;5(Suppl 4):S652-s6.
56. Davar D, Simonelli M, Gutierrez M, Calvo E, Melear J, Piha-Paul S, et al. 394 Interleukin-8–neutralizing monoclonal antibody BMS-986253 plus nivolumab (NIVO) in biomarker-enriched, primarily anti–PD-(L)1–experienced patients with advanced cancer: initial phase 1 results. Journal for ImmunoTherapy of Cancer. 2020;8(Suppl 3):A239.
57. Javaid F, Pilotti C, Camilli C, Kallenberg D, Bahou C, Blackburn J, et al. Leucine-rich alpha-2-glycoprotein 1 (LRG1) as a novel ADC target. RSC chemical biology. 2021;2(4):1206-20.
58. Munn LL, Jain RK. Vascular regulation of antitumor immunity. Science. 2019;365(6453):544-5.

Supplemental information

Table S1 | Overview evaluated immuno-oncology markers by Olink proteomic assay

Immuno-oncology markers							
IL-8	TNFRSF9	TIE2	MCP-3	CD40-L	IL-1a	CD244	EGF
PGF	IL-6	ADGRG1	MCP-1	CRTAM	CXCL11	MCP-4	TRAIL
FGF2	CXCL9	CD8A	CAIX	IFN-b	ADA	CD4	NOS3
IL-2	Gal-9	VEGFR-2	CD40	IL-18	GZMH	VEGFC	IL-12
CXCL1	TNFSF14	IL-33	TWEAK	CSF-1	PDCD1	FASLG	CD28
CCL19	MCP-2	CCL4	IL-35	Gal-1	PD-L1	CD27	CXCL5
IL-5	HGF	GZMA	HO-1	CX3CL1	CXCL10	CD70	IL-10
CD83	CCL23	CD5	CCL3	MMP7	ARG1	NCR1	DCN
TNFRSF21	TNFRSF4	MIC-A/B	CCL17	ANGPT2	PTN	CXCL12	IFN-γ
LAMP3	CASP-8	ICOSLG	MMP12	CXCL13	PD-L2	VEGFA	IL-4
IL-21	IL12RB1	IL-13	CCL20	TNF	KLRD1	GZMB	TNFRSF12A
PDGF subunit B	LAP TGF-b-1						

Table S2 | Patient characteristics OpACIN-neo

Characteristics	**Total cohort (n=86)**	
Institute		
Netherlands Cancer Institute	46	(53%)
Melanoma Institute Australia	38	(44%)
Karolinska Institute	2	(2%)
Age, years (median, IQR)	58, 45-65	
Sex		
Men	49	(57%)
Women	37	(43%)
Primary tumor stage		
T1a/b	29	(34%)
T2a/b	9	(10%)
T3a/b	14	(16%)
T4a/b	10	(12%)
Tx	24	(28%)
Treatment		
2x IPI 3 mg kg^{-1} + NIVO 1 mg kg^{-1} q3wk	30	(35%)
2x IPI 1 mg kg^{-1} + NIVO 3 mg kg^{-1} q3wk	30	(35%)
2x IPI 3 mg kg^{-1} q3wk directly followed by 2x NIVO 3 mg kg^{-1} q3wk	26	(30%)
Pathologic response		

Yes	64	(74%)
No	21	(24%)
NE[a]	1	(1%)
Recurrence[b]		
Yes	16	(19%)
No	70	(81%)
Alive[b]		
Yes	79	(92%)
No	7	(8%)

Percentages may not sum up to 100 because of rounding.
[a] Patient did not undergo surgery because of toxicity
[b] At data cutoff (14 February 2022), the median follow-up from data of registration was 47 months, with a minimum follow-up of 38 months for all patients alive.
IPI; ipilimumab, NIVO; nivolumab, IQR; interquartile range

Table S3 | Patient characteristics PRADO

Characteristics	**Total cohort (n=49)**	
Institute		
Netherlands Cancer Institute	49	(100%)
Age, years (median, IQR)	58, 52-68	
Sex		
Men	32	(65%)
Women	17	(35%)
Primary tumor stage		
T1a/b	6	(12%)
T2a/b	13	(27%)
T3a/b	13	(27%)
T4a/b	12	(24%)
Tx	1	(2%)
Unknown primary	4	(8%)
Pathologic response		
Yes	38	(78%)
No	11	(22%)
Recurrence[a]		
Yes	12	(24%)
No	37	(76%)
Alive[a]		
Yes	45	(92%)
No	4	(8%)

[a] At data cutoff (7 February 2022), the median follow-up from data of registration was 28.1 months, with a minimum follow-up of 23.4 months for all patients alive.
IQR; interquartile range

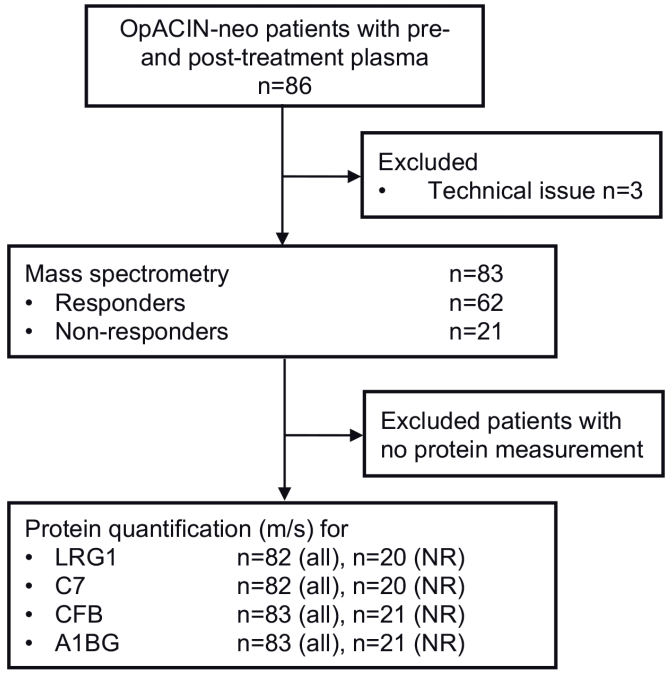

Figure S1 | Flowchart of patients OpACIN-neo study. Number of patients included for mass spectrometry. For every patient, two plasma samples were analyzed: one baseline samples (pre-treatment) sample and one post-treatment (after neoadjuvant ICB therapy) sample at week 6. Mass spectrometry data was available for 83 patients that had measurements for both pre-treatment and post-treatment samples. Patients with no measurement for certain proteins (e.g. LRG1 and C7) were excluded from the corresponding analysis. NR; non-responding patients

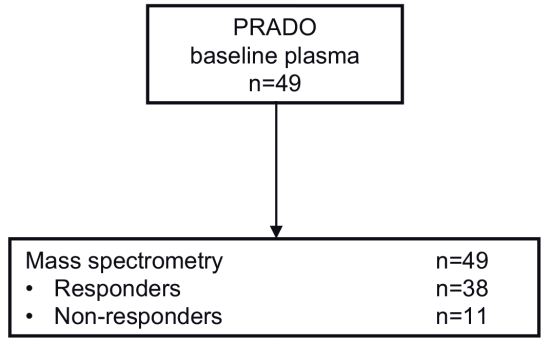

Figure S2 | Flowchart of patients PRADO study. A total of 49 patients from the PRADO study were included for mass spectrometry. The baseline (pre-treatment) plasma samples of patients were analyzed.

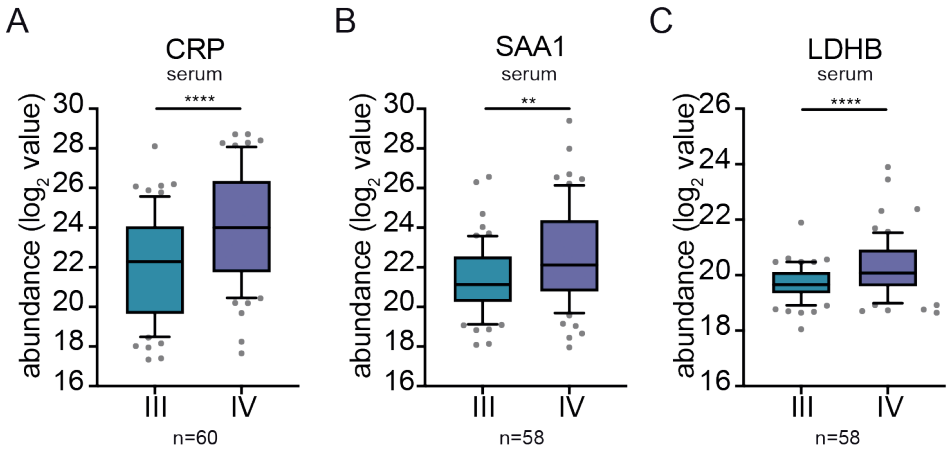

Figure S3 | SAA1, CRP and LDHB are associated with melanoma disease progression. Serum expression of **(A)** C-reactive protein (CRP) (n=60), **(B)** serum amyloid A1 (SAA1) (n=58) and **(C)** lactate dehydrogenase B (LDHB) (n=58) by patients with stage III disease that developed stage IV disease, as measured by mass spectrometry. A two-tailed paired Student's *t*-test was used to determine statistical significance between stage III and stage IV samples. **, $P < 0.01$, ****, $P < 0.0001$

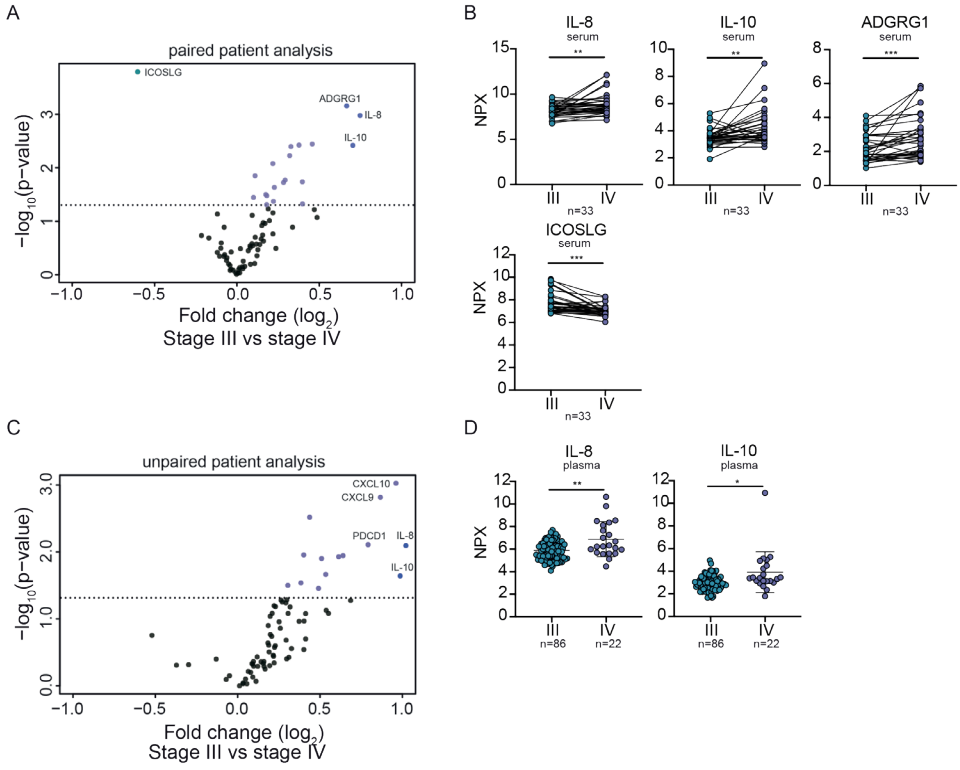

Figure S4 | Serum analysis using Olink proteomic assay. (A) Volcano plot showing differential marker expression of serum analysis using Olink immunoassay, comparing protein expression between matched patients with stage III and stage IV disease (n=33). Proteins with higher expression at stage III disease are displayed on the left, and proteins highly expressed at stage IV are displayed on the right. The protein fold change on a $\log_2$ scale is shown on the x-axis, with the significance indicated by the $-\log_{10}$ scale on the y-axis. The significance cut-off (*p*-value=0.05) is indicated with the black dotted line, showing significant increased proteins for stage III in blue and for stage IV in purple. A two-tailed paired Student's *t*-test was used to determine statistical significance between stage III and stage IV samples. **(B)** Normalized protein expression of significant proteins of (A) at stage III and stage IV for paired patients (n=33). Significance was assessed by a paired Student's *t*-test. **(C)** Volcano plot showing differential marker expression of plasma analysis using Olink immunoassay, comparing protein expression between patients with stage III (n=22) and stage IV (n=86) disease (not matched). Proteins higher expressed at stage III disease are displayed on the left, and proteins higher expressed at stage IV are displayed on the right. The protein fold change on a $\log_2$ scale is shown on the x-axis, with the significance indicated by the $-\log_{10}$ scale on the y-axis. The significance cut-off (*p*-value=0.05) is indicated with the black dotted line, showing significant increased proteins for stage IV in purple. A two-tailed unpaired Welch's *t*-test was used to determine statistical significance between stage III and stage IV samples. **(D)** Normalized protein expression for IL-8 and IL-10. Significance was assessed by an unpaired Welch's *t*-test between stage III and stage IV patients. *, $P<0.05$, **, $P<0.01$, ***, $P<0.001$

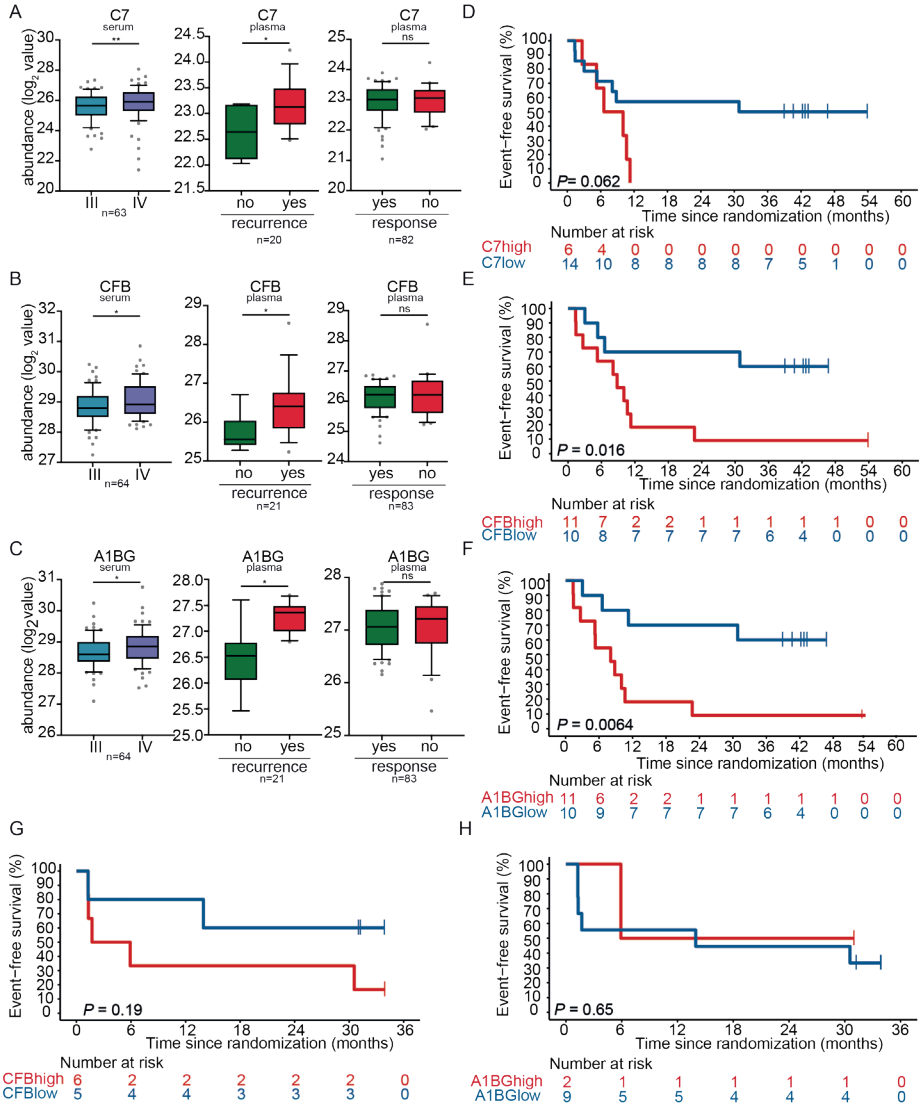

Figure S5 | Complement factor B (CFB), component 7 (C7) expression and alpha-1B-glycoprotein (A1BG) are increased upon melanoma progression and recurrence. (A-C) Normalized protein expression (log_2) values of **(A)** C7, **(B)** CFB and **(C)** A1BG, measured by mass spectrometry for matched stage III and IV patients (n=63 for C7, n=64 for CFB and A1BG), non-responsive patients of OpACIN-neo study (n=20 for C7, n=21 for CFB and A1BG) and all patients of the OpACIN-neo study (n=82 for C7, n=83 for CFB and A1BG). A two-tailed paired Student's *t*-test was used to determine statistical significance between stage III and stage IV samples. A two-tailed unpaired Student's *t*-test for comparing patients with and without a recurrence or response of the OpACIN-neo study, using a Welch's *t*-test when variances were significantly different. **(D-F)** A Kaplan Meier curve showing event-free survival (EFS) for non-responder patients of the OpACIN-neo study with either a high (red) or low (blue) expression of **(D)** C7, **(E)** CFB and **(F)** A1BG. *P* value was calculated using the log-rank test (two-sided) and significance is indicated. **(G-H)** A Kaplan Meier curve showing event-free survival (EFS) for non-responder patients of the PRADO study with either a high (red) or low (blue) expression of **(G)** CFB and **(H)** A1BG. *P* value was calculated using the log-rank test (two-sided) and significance is indicated. *, $P<0.05$, **, $P<0.01$

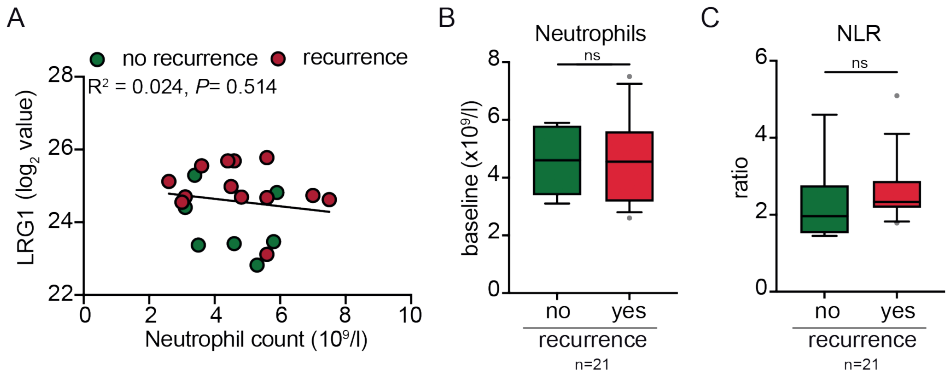

Figure S6 | Neutrophil count and neutrophil-to-lymphocyte ratio (NLR) are not associated with recurrence in non-responding patients. Analysis of pre-treatment samples of non-responding patients of the OpACIN-neo study. **(A)** Correlation between systemic normalized LRG1 expression and neutrophil count for patients without a recurrence (green dots) or without a recurrence (red dots). The correlation coefficient and *p*-value were computed using the Pearson correlation method. **(B)** Neutrophil count and **(C)** neutrophil-to-lymphocyte ratio at baseline for non-responding patients with or without a response (n=21). A two-tailed unpaired Student's *t*-test was used to compare patients with and without a recurrence.